Me_2SO-d_6) δ 3.33 (s, 3, CO_2CH_3), 3.38 (s, 3, CO_2CH_3), 6.27 (d, 1, aromatic, J = 9.3 Hz), 6.98–7.97 (m, 24, aromatic), 8.84 (d, 1, aromatic, J = 8.2 Hz); M^+· 688 (100).

Anal. Calcd for $C_{47}H_{32}N_2O_4$: C, 81.96; H, 4.68; N, 4.07. Found: C, 82.04; H, 4.87; N, 4.01.

Registry No. 3a, 6295-87-0; **3b**, 7583-90-6; **3c**, 7583-92-8; **6a**, 71870-12-7; **6b**, 71870-13-8; **6c**, 71870-14-9; **7a**, 71870-15-0; **7b**, 71870-16-1; **7c**, 71870-17-2; **8a**, 71870-18-3; **8b**, 71870-19-4; **8c**, 71870-20-7; **10a**, 71870-21-8; **10b**, 71870-22-9; **10c**, 71870-23-0; **11a**, 71870-24-1; **13**, 71870-25-2; **14**, 71870-26-3; **15**, 71870-27-4; **16**, 71870-28-5; **18**, 71870-29-6; **19** (R = CN), 71870-30-9; **19** (R = $COOCH_3$), 71870-31-0; **19** (R = COPh), 71870-32-1; **21**, 71870-33-2; **22**, 71870-34-3; **23**, 71870-35-4; **25** (R = $COOCH_3$), 71870-36-5; dibenzoylacetylene, 1087-09-8; *N*-phenylmaleimide, 941-69-5; 1-aminoquinolinium iodide, 7170-16-3; fumaronitrile, 764-42-1; dimethyl acetylenedicarboxylate, 762-42-5; 2-aminoisoquinolinium iodide, 40339-95-5; 7,8-dihydro-1,4-diphenylpyridazino[4′,5′:1,2]-pyrazolo[5,1-*a*]isoquinoline, 71870-37-6; 1,4-diphenylpyridazino-[4′,5′:1,2]pyrazolo[5,1-*a*]isoquinoline, 71870-38-7.

Theoretical Ab Initio SCF Investigation on the Photochemical Behavior of the Three-Membered Rings. 6. Aziridine[1]

B. Bigot,* A. Devaquet, and A. Sevin

Laboratoire de Chimie Organique Théorique,[2] Université Pierre et Marie Curie, 75230 Paris Cedex 05, France

Received July 24, 1979

Ab initio SCF–CI methods have been used to calculate the potential energy curves corresponding to the ground and low-lying states of the aziridine system when various reaction paths are simulated. They concern three topics: the CC and CN bond rupture ring opening, the formation of carbene and nitrene, the NH bond rupture. The main results are the following: in the gas phase, the CN ring opening is favored while in protic condensed media CC ring opening competes; the nitrene formation is easier in a two-step procedure than in a synchronous two-bond scission while it is the reverse for carbene formation; the unimolecular NH bond rupture is not a primary process in the formation of molecular hydrogen from aziridine. The difference between gas-phase and condensed-protic-phase reactivity is explained by the role played by Rydberg and hydrogen-bond electronic-transfer states.

The photochemical behavior of aziridine and aziridine derivatives is rather complex as shown by numerous experimental works reported in the literature.[3] The nature and distribution of the resulting products strongly differ whether the reaction is carried out in gas or condensed phase.

In the gas phase, aziridine breaks into a variety of products such as molecular hydrogen and nitrogen, ethylene, ammonia, saturated hydrocarbons, and a dimer of the ethylenimino radical.[4,5] Their relative abundance sharply depends on experimental conditions. For example, under static conditions,[5a,c] a great amount of ammonia is produced, but no nitrile compounds are formed (the last assertion is denied by some authors).[3b,6] In a fast-flow system,[5b] however, nitrile compounds have been clearly identified, and the ammonia production is less than in the preceding conditions. Various primary processes[4,5] have been proposed to explain the nature and relative importance of the photodecomposition products, including nitrene extrusion and NH bond rupture. No process, however, involves CC bond rupture.

In the condensed phase, particularly in alcoholic solution, two primary processes are well documented. The first one is deamination[7] which corresponds to the nitrene extrusion previously mentioned for the gas-phase reaction. The second corresponds to a CC bond rupture ring opening.[8] It yields one to three dipolar ylides which can be trapped with various dipolarophiles,[8a] exhibit photochromic properties,[8b] or undergo further fragmentation leading to carbene and imine species.[8c] These fragments differ from those obtained in the gas phase. It appears that polar solvents favor the last evolution—CC bond rupture.

Thus, although several extended experimental studies have been devoted to the subject, the photochemical primary processes of aziridine are not fully ascertained, and the influence of factors such as substitution or solvation is not completely understood.

The subject of this paper is to try to get some new insights on the intimate behavior of the photochemically excited aziridine system by theoretical ab initio SCF–CI investigation. The reactions which will be considered are depicted in Figure 1.

The first simulated transformations are the openings of the three-membered ring by CC bond rupture. Indeed, according to Woodward–Hoffmann denomination,[3] three main modes are to be considered: the face to face (path a), the conrotatory (path b), and the disrotatory (path c) processes. The first mode leads to the formation of intermediate I′ while the last two ones lead to the formation of the same planar intermediate (I). In order to solve the dichotomy concerning the CC reactivity in the gas and in the protic condensed phases, paths a′, b′ and c′ have been simulated. They represent the same transformations as paths a, b, and c, respectively, in presence of a proton in

(1) Preceding paper: B. Bigot, D. Roux, A. Devaquet, and A. Sevin, *J. Am. Chem. Soc.*, **101**, 2560, 1979.

(2) This laboratory is also part of the CNRS (ERA No. 549).

(3) For a review, see: (a) N. R. Bertoniere and G. W. Griffin, *Org. Photochem.*, **3**, 115 (1973); (b) S. Braslavsky and J. Heicklen, *Chem. Rev.*, **4**, 473 (1977); (c) O. C. Demer and G. E. Hamm, "Ethyleneimine and Other Aziridines", Academic Press, New York, 1969.

(4) (a) M. Kawasaki, T. Ibuki, and J. Takezaki, *J. Chem. Phys.*, **59**, 6321 (1973); M. Kawasaki, M. Iwasaki, and T. Tanaka, *ibid.*, **56**, 6328 (1973); M. Kawasaki, Y. Hirato, and I. Tanaka, *ibid.*, **59**, 648 (1973); M. Kawasaki, T. Ibuki, M. Iwasaki, and Y. Takesaki, *ibid.*, **59**, 2076 (1973); (b) A. A. Scala and D. Salomon, *ibid.*, **65**, 4455 (1976).

(5) (a) C. Luner and H. Gesser, *J. Phys. Chem.*, **62**, 1148 (1958); (b) A. Jones and F. P. Lossing, *Can. J. Chem.*, **45**, 1685, (1967); (c) R. F. Klemm, *ibid.*, **43**, 2633 (1965); **45**, 1685 (1967); (d) A. B. Callear and J. C. Mc Gurk, *J. Chem. Soc., Faraday Trans. 2*, **68**, 289 (1972).

(6) D. W. Cornell, R. S. Berry, and W. Lwowski, *J. Am. Chem. Soc.*, **88**, 544 (1966).

(7) A. Padwa and L. Hamilton, *J. Am. Chem. Soc.*, **87**, 1821 (1965); **89**, 102 (1967); **90**, 2442 (1968).

(8) (a) H. W. Heine and R. E. Peavy, *Tetrahedron Lett.*, 3123 (1965); R. Huisgen, W. Scheer, and H. Huber, *J. Am. Chem. Soc.*, **89**, 1753 (1967); R. Huisgen and H. Mäder, *ibid.*, **93**, 1777 (1971); H. Hermann, R. Huisgen, and H. Mäder, *ibid.*, **93**, 1779 (1971); (b) H. Nosaki, S. Fujita, and R. Noyori, *Tetrahedron*, **24**, 2193 (1968); (c) M. A. Trozzolo, "Photochromism", Wiley-Interscience, New York, 1971.

(9) R. B. Woodward and R. Hoffmann, *Angew. Chem., Int. Ed. Engl.*, **8**, 781 (1969).

0022-3263/80/1945-0097$01.00/0

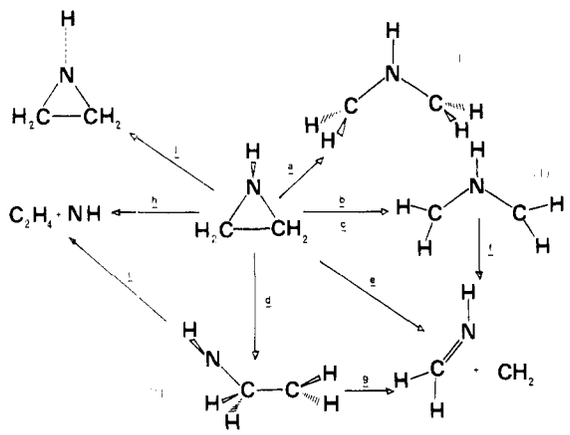

Figure 1. Scheme presenting the different reaction paths for the aziridine system presently studied.

the vicinity of the nitrogen atom.

The second primary process is the CN bond rupture ring opening (path d). It leads to the formation of the intermediate II.

The fragmentations into carbene and imine have been simulated by three reaction paths. The first one is a direct simultaneous two-bond scission from aziridine (path e). The second and third ones are two-step reaction paths. They involve, in a first step, the previously described formation of the intermediates I and II, respectively. In a second step, the CN (path f) or CC (path g) bond rupture of these intermediates occurs.

The fragmentations into ethylene and nitrene have been simulated by the two following reaction paths: a simultaneous two-bond scission from aziridine (path h) and a two-step process involving the intermediate II (path d followed by path i).

Finally, the NH (path j) bond rupture has been investigated in order to explain the molecular hydrogen formation in the gas phase.

In all the transformations reported here, the values of the geometrical parameters describing the systems undergo linear variations between the initial and the final points.

This procedure is adapted to our purpose which is to draw qualitative potential energy curves (PECs) for these reaction paths, depicting the main features (energy barrier, potential wells, near-touching surfaces) which govern[10] the photochemical reactivity of the species.

For this purpose, for each of the different reaction paths, the MO and state diagrams have been studied by using the natural MO correlation concept.[11] To check precisely the conclusions to which they lead, we have performed the corresponding PEC calculations of the ground state (GS) and low-lying excited states using an ab initio SCF–CI method described elsewhere.[12]

Let us recall that this complete procedure only intends to provide qualitative—or more exactly semiquantitative–information relative to the shapes of the different PECs involved in a reaction path. Consequently, the chemical

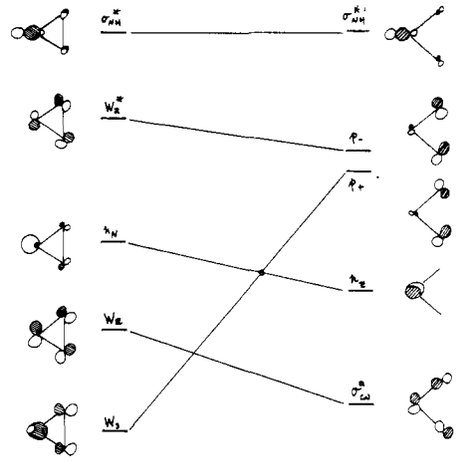

Figure 2. Natural MO correlation diagram in the face to face CC bond rupture ring opening (path a) leading to intermediate I′. The circle represents the avoided crossing at the SCF level.

conclusions which will be drawn afterward lay rather on the consideration of the PEC shapes than on numerical calculated values, which are only indicative of an order of magnitude.

Aziridine: Calculated Properties

Various calculations on aziridine, in its ground state, have been reported in the literature.[15] We have adopted the geometry determined by Pople et al.,[15d] which is in correct agreement with experimental findings.[16]

Let us first describe the MOs which will be of main concern in the following discussions (see Figure 2). The occupied orbitals are, by order of increasing energy, W_S and W_A, the symmetrical and antisymmetrical Walsh bonding orbitals,[17] and n_N, so called owing to its lone-pair character. The unoccupied orbitals are W_A*, the antibonding Walsh orbital, and σ_{NH}*.

The first calculated vertical singlet excitation $^1(n_N \rightarrow W_A^*)$ lies at 11.2 eV (110 nm). The corresponding triplet lies at 9.20 eV (133 nm). For the estimation of the reliability of these calculated values, let us compare them with experimental results.[18] The first absorption band appears at 6.94 eV (178 nm) and the next one at 8.55 eV (144 nm). They are both associated with Rydberg transitions. The first valence transition is attributed to the strong absorption band lying at 10.5 eV (117 nm). Considering that our calculations do not take into account Rydberg transition, the present results appear as a correct estimation of the position of the first valence excited states.

In a first approximation, the low-lying Rydberg states could be considered as "reservoir states"[19] which are likely to populate the reactive states via crossings with their PECs (vide infra).

CC Rupture Ring Opening: Paths a, b, c, a′, b′, and c′

Let us first consider nonprotonated aziridine. Three modes of CC rupture ring opening having been investi-

(10) J. Michl, *Mol. Photochem.*, 4, 243 (1972); 4, 257 (1972); 4, 287 (1972); *Top. Curr. Chem.*, 46, 1 (1974).

(11) (a) A. Devaquet, A. Sevin, and B. Bigot, *J. Am. Chem. Soc.*, 100, 2009 (1978); (b) B. Bigot, A. Sevin, and A. Devaquet, paper presented at the 7th Symposium on Photochemistry. Louvain, France, July 1978.

(12) B. Bigot, A. Sevin, and A. Devaquet, *J. Am. Chem. Soc.*, 100, 2639 (1978). It uses the series of GAUSSIAN 70 program[13] in the STO-3G basis option.[14] The CI segment of the calculation involves the singly and doubly excited configurations obtained by promoting one or two electrons from the six highest occupied to the four lowest unoccupied MOs.

(13) W. J. Hehre, W. A. Lathan, R. Ditchfield, M. D. Newton, and J. A. Pople, *QCPE*, No. 236, Indiana University, Bloomington, Indiana.

(14) W. J. Hehre, R. F. Stewart, and J. A. Pople, *J. Chem. Phys.*, 51, 2657 (1969).

(15) (a) J. M. Lehn, B. Munsch, P. Millié, and A. Veillard, *Theor. Chim. Acta*, 13, 313 (1969); (b) A. Veillard, J. M. Lehn, and B. Munsch, *ibid.*, 9, 275 (1968); (c) B. Levy, P. Millie, J. M. Lehn, and B. Munsch, *ibid.*, 18, 143 (1970); (d) W. A. Lathan, L. Radom, P. C. Hahiharan, W. J. Hehre, and J. A. Pople, *Top. Curr. Chem.*, 40, 1 (1973); (e) E. R. Talaty and G. Simons, *Theor. Chim. Acta*, 48, 331 (1978).

(16) B. Bak and S. Skahrup, *J. Mol.* Struct., 10, 385 (1971).

(17) A. D. Walsh, *Nature (London)*, 159 (1947).

(18) H. Basch, M. B. Robin, N. A. Kuebler, C. Baker, and D. W. Turner, *J. Chem. Phys.*, 51, 52 (1969).

(19) A. Sevin, B. Bigot, and A. Devaquet, *Tetrahedron*, 34, 3275 (1978).

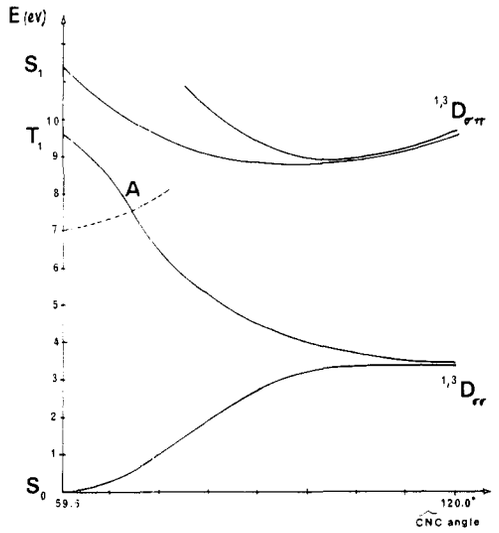

Figure 3. Calculated potential energy curves in path a. The dashed lines represent the estimated behavior of the Rydberg state potential energy curves.

gated. They correspond to a simulation of the CC bond reactivity in the gas phase.

The face to face mode (path a) leads to the formation of the intermediate I',[20] for which the value of the CNC angle has been fixed at 120°. Along the reaction path, the initial symmetry plane is preserved.

The natural MO correlation diagram (Figure 2) shows that no HOMO–LUMO crossing occurs. Only crossings between occupied orbitals intervene. The quasi-degenerate (p_+, p_-) pair of orbitals is characteristic of a homosymmetrical diradical.[21] Thus, the first four electronic states of intermediate I' are the diradical states $^{1,3}D_{\sigma\sigma}$ and $^{1,3}D_{\sigma\pi}$. The first singlet, which lies 3.4 eV above the aziridine ground state, corresponds to the mixing of configurations $(p_+)^2$ and $(p_+ \rightarrow p_-)^2$ with a dominant contribution of the first one. The first triplet which corresponds to the ($p_+ \rightarrow p_-$) configuration is degenerate with the preceding singlet. The next singlet and triplet states correspond to the excitation ($n_z \rightarrow p_-$), and both lie around 9.8 eV above aziridine ground state (GS).

It follows that the S_0 state of aziridine correlates directly with $^1D_{\sigma\sigma}$ and the $^{1,3}(n_N \rightarrow W_A^*)$ (S_1 and T_1) states correlate with $^{1,3}D_{\sigma\pi}$. As for the $^3D_{\sigma\sigma}$ state, it correlates with a high-lying triplet state of aziridine ($W_S \rightarrow W_A^*$). An avoided crossing of the triplet correlation lines results. This avoidance is considered to be important since the orbitals (n_N, W_S) which determine it[22] are localized in the same spatial region. The calculated PEC shapes of Figure 3 are obtained. They are in correct agreement with the preceding qualitative analysis.

Let us now consider the two different modes (disrotatory and conrotatory) of CC rupture which lead to the planar intermediate I.[23] In the disrotatory process (path c), a symmetry plane is preserved along the reaction path. In the conrotatory process (path b), no symmetry element exists.

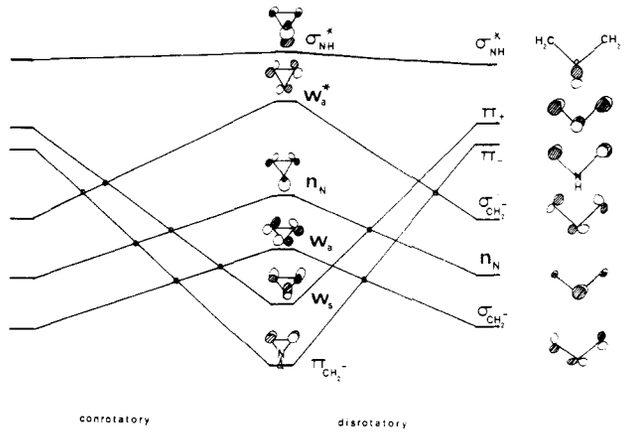

Figure 4. Natural MO correlation diagrams in the disrotatory (right part) and conrotatory (left part) CC bond rupture ring opening (paths c and b, respectively). The circles represent the avoided crossings at the SCF level.

For both modes, the transformation of the MO framework depends on two factors: the breaking of the CC bond and the rotation of the methylene groups. In conformity with previous calculations on cyclopropane,[24] it appears that the processes are dominated by the CC elongation and that the methylene rotations intervene only once the CC rupture is practically achieved.

These elements allow us to consider the CC bond breaking as the governing factor which determines the MO correlation. Thus, by use of the phase and location conservation rules,[11] the natural MO correlation diagrams of Figure 4 are obtained. They are very similar except that, at the SCF level, all the crossings are avoided in the conrotatory mode, while a few remain allowed in the disrotatory mode, particularly the HOMO–LUMO crossing.

Let us note that the relative position of the π^+ and π^- MOs are in conformity with Hoffmann's considerations on the similar EE form of trimethylene.[25]

The first electronic states of intermediate I are the singlet–triplet pair $^{1,3}D_{\pi\pi}$, characteristic of a homosymmetrical diradical defined on the (π^+, π^-) quasi-degenerate orbital pair. These states lie respectively at 2.10 and 3.20 eV above the aziridine GS. Next, the corresponding Z_1 and Z_2 zwitterionic states come at 9.4 and 11.4 eV, respectively.

In the scope of the natural-correlation approach, the primitive state diagrams are identical in the two ring-opening modes.

Two facts will intervene to determine the particular shapes of the various PECs for each mode. The first one is the number of avoided crossings: within a given spin multiplicity, all the crossings are avoided in path b while some remain allowed in path c. The second fact is that a crossing is qualitatively less strongly avoided if it intervenes only at the state level than if it has already been taken into account at the MO level.

The calculated curves confirm this analysis. For example, the maximum on the S_0 PEC lies at 3.8 eV above the aziridine GS in the conrotatory mode but at 4.6 eV in the disrotatory one (Figures 5 and 6).

Let us now compare the three different modes.

Thermally, in the scope of our model of linear deformation, the easiest way is the face to face process. However, structure I' is not a stable intermediate since no energy barrier prevents it from reclosing to aziridine. A possibility for reaching stable structure I is to begin the

(20) The structure of intermediate I' is defined as follows: the two carbon atoms and the NH fragment are located in a same plane; the HCH bissectors are colinear with the CN bonds; CN = 1.48 Å, CNC = 120°, and HCH = 120°.

(21) L. Salem and C. Rowlands, *Angew. Chem., Int. Ed. Engl.*, 11, 92 (1972).

(22) L. Salem, C. Leforestier, G. Segal, and R. Wetmore, *J. Am. Chem. Soc.*, **96**, 3486 (1974).

(23) The structure of intermediate I is defined as follows: all the atoms are in a same plane; the HCH bissectors are colinear with the CN bonds; CN = 1.36 Å, CNC = 120°, and HCH = 120°.

(24) X. Chapuisat and Y. Jean, *J. Am. Chem. Soc.*, **97**, 6325 (1975), and references therein.

(25) R. Hoffmann, *J. Am. Chem. Soc.*, **90**, 1475 (1968).

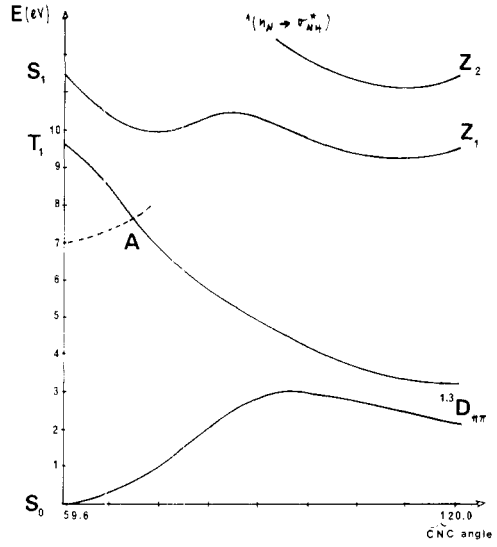

Figure 5. Calculated potential energy curves in path b. The dashed lines represent the estimated behavior of the Rydberg state potential energy curves.

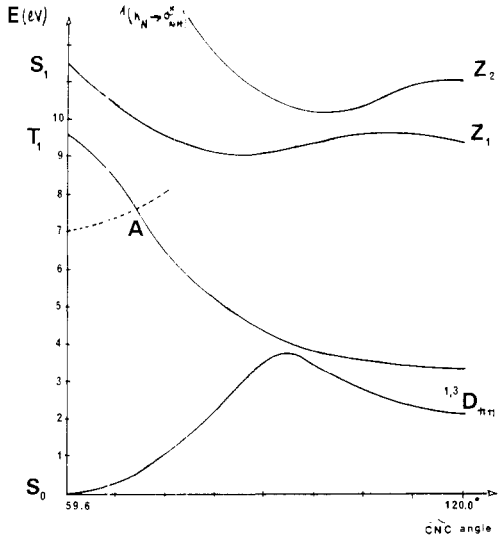

Figure 6. Calculated potential energy curves in path c. The dashed lines have the same meaning as in Figure 5.

process by the face to face motion up to a value of the CNC angle of around 100° and then to pursue it by the conrotatory rotation of the methylene groups. The energy barrier can be estimated at 2.9 eV, in correct agreement with experimental findings.[26]

Photochemically, the T_1 state is reactive in each case. The S_1 state appears much less reactive. In path a, the system can only decay from the S_1 to the S_0 PEC and reclose to aziridine. In paths b and c no easy way appears. However, the high-energy position of these states prevents any direct experimental population, and consequently the CC bond rupture does not appear as an easy process under photochemical conditions in the gas phase.

Could the consideration of Rydberg states modify these conclusions?

The main contributions to the lowest Rydberg states are excitation from the n_N to the $3s_N$ or $3p_N$ nitrogen orbitals.[18] They do not involve a bonding valence MO. Thus, the behavior of the corresponding PECs may be estimated to be roughly parallel to that of the S_0 PEC. If one superposes the estimated PECs on the preceding calculated diagram, one notes that they will cross the dissociative valence PECs at points so high in energy (more than 15 kcal/mol) that no important qualitative change would result for the preceding conclusions—the CC bond rupture is not a favorable photochemical process.

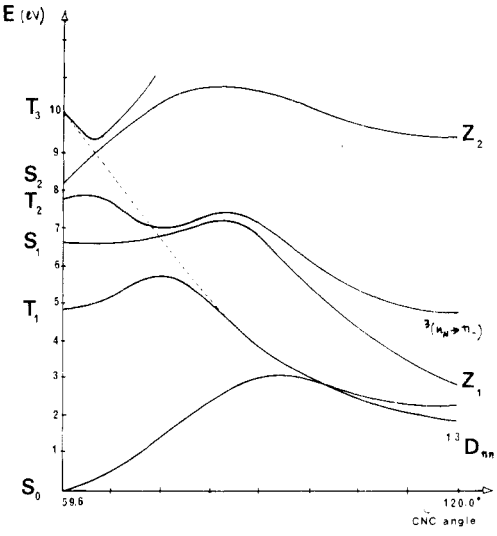

Figure 7. Calculated potential energy curves in the conrotatory CC ring opening of protonated aziridine (path b'). The dashed lines represent the observed curve for the T_1 state in the nonprotonated case (see Figure 5).

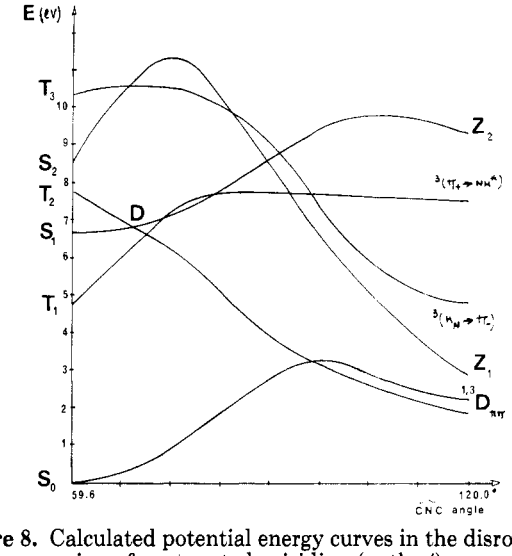

Figure 8. Calculated potential energy curves in the disrotatory CC ring opening of protonated aziridine (path c').

What are the differences in protic condensed media? For simulating the process in such a case, a proton has been added to the aziridine system. It lies 1.5 Å in a vertical direction from the nitrogen atom.[32]

The protonation will have two influences. First, it will stabilize the zwitterionic Z_1 state of the open form I. Second, it will lead to the existence of low-lying excited states corresponding to the electronic transfer from bonding valence orbitals along the CC bond to the N···H bond. During the ring opening, these states will be less destabilized than the corresponding Rydberg states considered in absence of protonation. The latter reduce the bonding character along the broken bond while the former do not affect the bonding framework as it is in the S_0 state. The result is that the corresponding PECs will cross the reactive T_1–$^3D_{\pi\pi}$ PEC in a region that is energetically more easily accessible. The calculated curves depicted in Figures 7 and 8 can be analyzed within this scheme.

(26) J. Meier, F. Akermann, and H. H. Gunthard, *Helv. Chim. Acta*, 51, 1686 (1968).

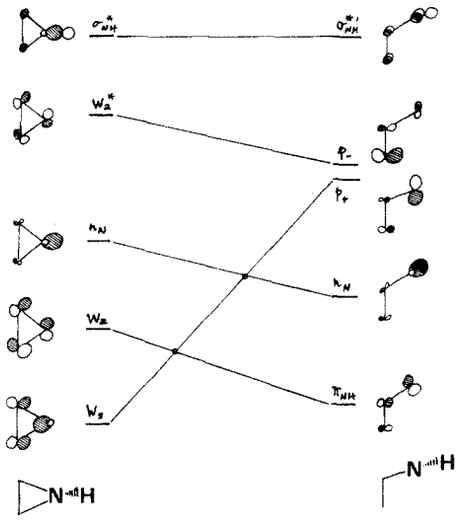

Figure 9. Natural MO correlation diagram in the CN bond rupture ring opening (path d). The circles represent the avoided crossings at the SCF level.

Let us consider, for example, the triplet PECs. The $^3(n_N \rightarrow W_A^*)$ state of aziridine intends to correlate with the $^3D_{\pi\pi}$ state of structure I (dashed lines on Figure 7). It would cross the $^3(W_s \rightarrow \sigma_{N\text{-}H}^*)$ and $^3(W_A \rightarrow \sigma_{N\text{-}H}^*)$ PECs. These two crossings are avoided in the conrotatory process while only the upper one is so in the disrotatory one. The full lines curves result.

The reactivity is strongly modified if we make a comparison with the gas phase. In the disrotatory mode, two reactive ways can now be considered. The first one involves the lowest singlet state. It requires an intersystem crossing at point D, after overcoming an energy barrier of less than 10 kcal/mol. This value is compatible with the estimated lifetime of such a singlet state.[11a] Let us note that the energy position of this singlet (6.6 eV) is in the range of the experimental active radiation (200 nm or 6.2 eV).[8] The second one is the second triplet $^3(W_A \rightarrow \sigma_{N\text{-}H}^*)$ which leads directly to the $^3D_{\pi\pi}$ state. In the conrotatory mode, no comparable easy way exists.

In condensed protic media, the preceding study confirms that thermally the CC ring opening is preferentially conrotatory while photochemically it is disrotatory.

Let us now consider the ring opening via CN bond rupture.

CN Rupture Ring Opening: Path d

The geometry of structure II has been fully optimized,[27] with the value of the CCN angle fixed at 109°. The N-linked hydrogen lies out of the CCN plane. Thus, the present opening resembles a face to face process. It is the reason why the natural MO correlation diagram (Figure 9) is similar to that observed in the face to face CC rupture (Figure 2).

The first electronic states of the intermediate II are the S_0 and T_1 diradical states. They are quite degenerate in energy and lie around 2.0 eV above the aziridine GS. The following states (S_1 and T_2), which correspond to the excitation of one electron from n_N to the (p_+, p_-) pair of orbitals, lie around 3.0 eV above the S_0 and T_1 states. If we compare this with the CC face to face process, it is clear that S_0 and T_1 correspond the $^{1,3}D_{\sigma\sigma}$ states and S_1 and T_2 to the $^{1,3}D_{\sigma\pi}$ states. The state correlations are the same in both cases and justify the similarity of the calculated curves (Figure 10).

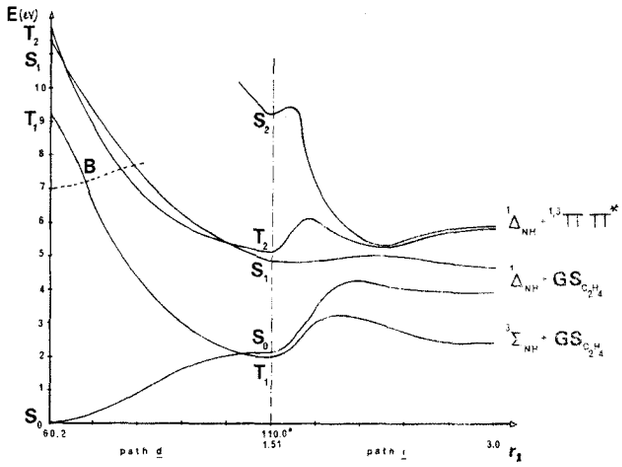

Figure 10. Calculated potential energy curves in the fragmentation of aziridine into nitrene and ethylene by a two step process. The left part of the figure represents the CN ring opening (path d) and the right one the CN bond rupture of the intermediate II (path i). The dashed lines are relative to the estimated behavior of the Rydberg state potential energy curves.

However, two differences intervene when comparing the CC and CN cleavages. First, the $^1(n_N \rightarrow W_A^*)$ state is now potentially reactive while only the corresponding triplet is reactive in the CC rupture. It leads directly to the low-lying S_1 state of the intermediate II. Second, the Rydberg states constitute easy ways to reach the dissociative PECs. Indeed, keeping the hypothesis that Rydberg states have PECs parallel to the S_0 PEC, one finds that the intersection points (B in Figure 10, A in Figure 3) are more easily accessible in the CN rupture (5 kcal/mol) than in the CC one (15 kcal/mol). These two differences have their origin in the fact that the CN bond is weaker than the CC one—the S_0, T_1, S_1, and T_2 states of II are more stable than the $^{1,3}D_{\sigma\sigma}$ and $^{1,3}D_{\sigma\pi}$ states of I'.

Let us note, otherwise, that no energy barrier prevents the ring reclosure of the intermediate II. This fact can strongly reduce the thermal as well as the photochemical efficiency of the CN bond rupture.

Formation of Carbene and Imine: Paths e, f, and g

As already mentioned, three different reaction paths may be considered for the formation of carbene and imine from aziridine.

The first one is the simultaneous two-bond scission (path e). The initial HCH angle of 116° has been kept constant for the methylene fragment all along the reaction path. It represents an intermediate situation between the optimal values of the different $^3B_1$ and $^1A_1$ lowest states of methylene.[28]

The natural MO correlations are depicted in Figure 11. Numerous crossings occur, among them a HOMO–LUMO

(27) The structure of intermediate (II) is defined as follows where CN = 1.51 Å, CC = 1.42 Å, CNH = 102°, and NCC = 109°.

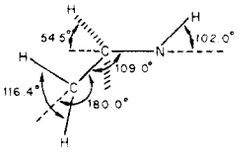

(28) J. F. Harrison, *Acc. Chem. Res.*, **7**, 378 (1974). R. R. Lucchese and H. F. Schaefer III, *J. Am. Chem. Soc.*, **99**, 6745 (1977), and references, therein. The lowest states of the imine–methylene system for a CC distance of 2.8 Å are the $^3B_1$, $^1A_1$, and $^1B_1$ methylene states and the imine ground state. $^1A_1$ and $^1B_1$ are around 0.3 and 2.8 eV, respectivelly, above $^3B_1$.

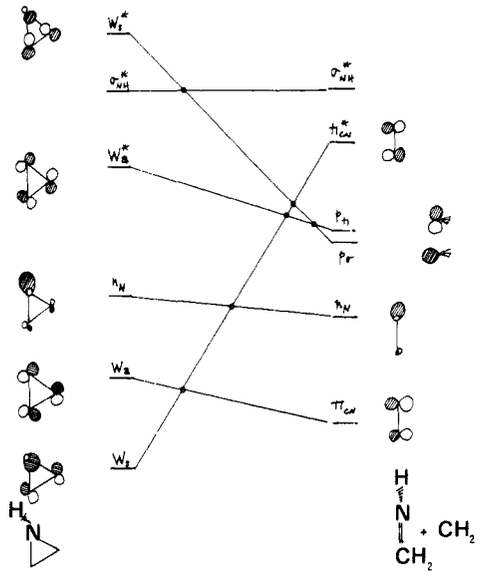

Figure 11. Natural MO correlation diagram in the fragmentation of aziridine into carbene and imine in a concerted process (path e). The circles represent the avoided crossings at the SCF level.

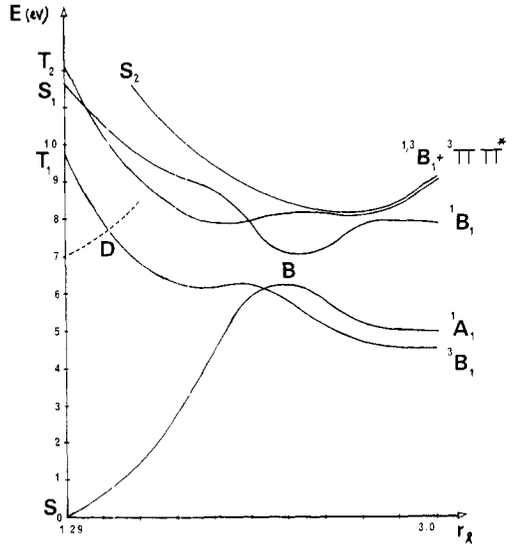

Figure 12. Calculated potential energy curves in the fragmentation of aziridine into carbene and imine in one step (path e). The reaction coordinate is the distance between the carbene carbon atom and the CN bond. The dashed lines are relative to the estimated behavior of the Rydberg state potential energy curves.

crossing. Without analyzing in detail the resulting state diagram, one can predict avoided crossings and corresponding extremes along the PECs of all the low-lying states. The calculated curves illustrate this point (Figure 12).

Thermally, a 6.20-eV energy barrier prevents any possibility for aziridine from breaking this way.

Photochemically, the $^{1,3}(n_N \rightarrow W_A^*)$ singlet and triplet may be considered as potentially reactive states. On the one hand, from S_1, the system can reach the region of the minimum B and then decay from S_1 to the near-touching S_0 PEC. On the other hand, it appears that the system is able to overcome the weak barrier which is encountered on the T_1 PEC.

However, if one considers that these valence states are not experimentally accessible, one must take into account the reactivity of the lower Rydberg states. The study of the estimated PECs of these states (dashed lines) shows that their efficiency is very low since the intersecting point

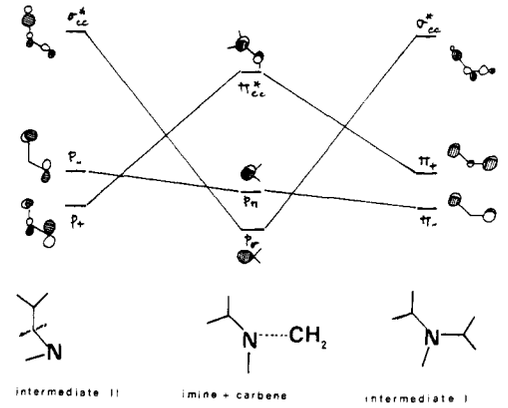

Figure 13. Natural MO correlation diagrams in the second step of the fragmentation of aziridine into carbene and imine. The left part is relative to path g (involving intermediate II) and the right part is relative to path f (involving intermediate I).

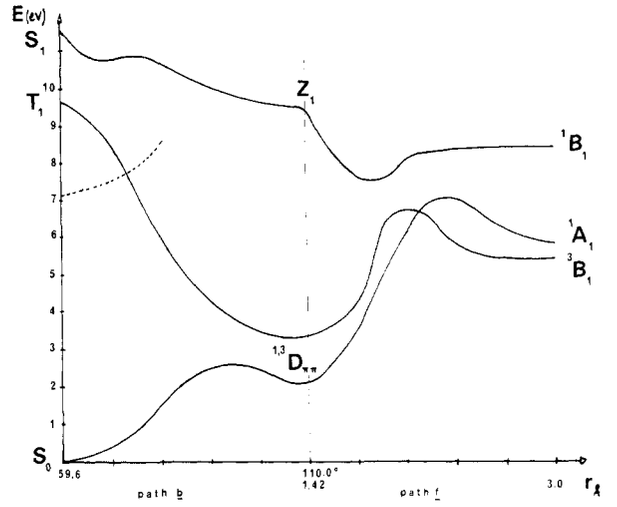

Figure 14. Calculated potential energy curves in the fragmentation of aziridine into carbene and imine in a two-step process involving intermediate I. The left part is relative to path b and the right part to path f.

D is around 20 kcal/mol above the vertical transition.

Let us now consider the two-step processes. The first one involves the formation of intermediate I as a primary step while the second involves the formation of intermediate II. In a second step, a CC bond is broken while the imine fragment reorganizes. In both cases, HOMO–LUMO crossing occurs in the natural MO correlation diagram (Figure 13). At the SCF level, these crossings are avoided in path g, since no symmetry element is preserved, while they remain allowed in path f. Thus no monotonic correlation line links the different lowest states of the final imine–methylene system to those of the intermediates I or II.

This situation leads to the existence of extremes along the PECs of lowest energy. Since the avoided crossings are already taken into account at SCF–MO level for path g, the resulting extremes are expected to be less prominent along this path than along path f where the avoidances only occur at the state level.

This situation is confirmed by the calculated curves (Figures 14 and 15).

Thermally, the reaction appears to be as difficult as that in the simultaneous two-bond scission (5.4 eV for path d + g, 7.0 eV for path b + f.

Photochemically, no low-energy reactive channel is found. Indeed, the energy barriers which appear in the second step (ca. 3.3 eV) are difficult to overcome even if

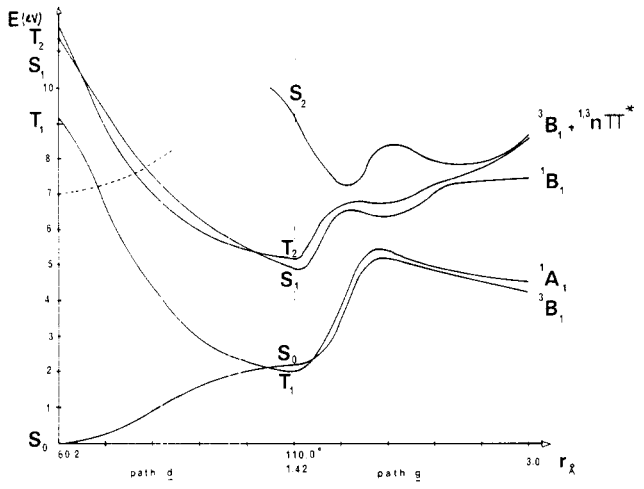

Figure 15. Calculated potential energy curves in the fragmentation of aziridine into carbene and imine in a two-step process involving intermediate II. The left part is relative to path d and the right part to path g.

one considers that the system has gained an important internal energy during the first step and that it has no time to dissipate it in totality to the surroundings. If one estimates that the first step has occurred via Rydberg or N···H transfer states, the maximal value of the available internal energy is around 3.0 eV.

In conclusion, one must consider that the imine–methylene fragmentation is unlikely in the gas phase whatever the reaction path. In the condensed protic phase, the only photochemical reactive channel is the simultaneous two-bond scission from N···H transfer states which cross the dissociative valence triplet state leading to the $^3B_1$ state of the imine–methylene system.

Considering now the addition of carbene to imine (reverse of the previous process) to form aziridine, various reactive channels are likely. The first ones involve the $^1A_1$ state of methylene. Whatever the reaction path, these channels require the overcoming of a comparable energy barrier. The second ones involve the second singlet state, $^1B_1$. The system spontaneously reaches a potential well from which an effective decay to the S_0 surface is likely to occur. In the two cases, no clear-cut difference distinguishes the two-bond scission from the two-step processes, contrary to the triplet $^3B_1$ channel. The $^1B_1$ singlet leads to the formation of a stable intermediate (I or II) which can easily reclose to aziridine in the two-step processes while it requires a difficult intersystem crossing (point C, Figure 13) in the concerted mode. These results are in agreement with the experimental findings relative to the similar ethylene–methylene[29] system.

Formation of Nitrene and Ethylene: Paths h and i

The formation of nitrene has been simulated by following two different reaction paths. The first one is a direct simultaneous two-bond scission from aziridine (path h). A symmetry plane is preserved all along the reaction path, and the NH bond remains out of the CCN plane. The second is a two-step procedure involving in a first step the formation of the intermediate II (path d) which then cleaves into nitrene and ethylene (path i).

The natural MO correlation diagram of Figure 16 reveals that no HOMO–LUMO crossing occurs along path h. Only crossings between occupied or between unoccupied orbitals

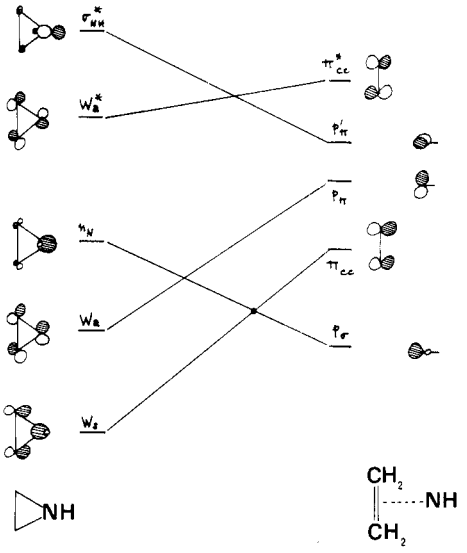

Figure 16. Natural MO correlation in the fragmentation of aziridine into ethylene and nitrene in a concerted process (path h). The circle represents the avoided crossing at the SCF level.

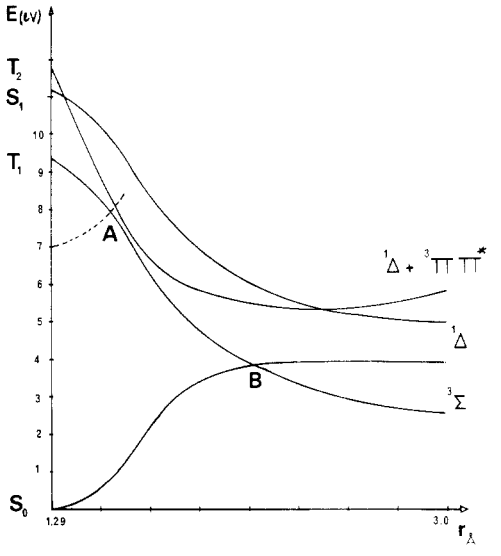

Figure 17. Calculated potential energy curves in the fragmentation of aziridine into ethylene and nitrene in a concerted process (path h). The reaction coordinate is the distance between the nitrogen atom and the CC bond.

intervene. The GS of aziridine thus correlates directly with the first singlet state of the final system—nitrene in its $^1\Delta \equiv (p_\sigma^2 p_\pi^2)$ state and ethylene in its GS. The $^{1,3}(n_N \rightarrow W_A^*)$ states of aziridine are in correlation with charge-transfer states $^{1,3}(p_\sigma \rightarrow \pi_{CC}^*)$. Reciprocally, the $^{1,3}(p_\pi \rightarrow p_\pi')$ states of the final system correlate with high-lying excited states of aziridine—$^{1,3}(W_A \rightarrow \sigma_{NH}^*)$. The two resulting crossings are avoided, but they are of moderate consequence to the corresponding PECs as is shown on the calculated curves of Figure 17.

The first singlet and triplet states of aziridine appear as potential reactive states which lead directly to the fragmentation. However, once again, this conclusion must be tempered by the fact that these states are experimentally difficult to populate. If one considers the Rydberg states (dashed lines), their reactivity is seen to be low since the intersecting point of their PECs with those of the dissociative valence states is high in energy (more than 20 kcal/mol).

Let us now consider the reaction path i. The natural MO correlation diagram must be very similar to those represented in Figure 14. Particularly, a HOMO–LUMO

(29) W. Kirmse, "Carbene Chemistry", Academic Press, New York, 1971, Chapter 8.

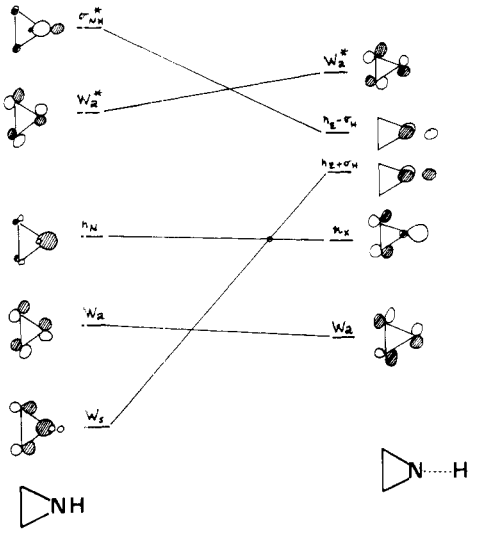

Figure 18. Natural MO correlation diagram in the NH bond rupture (path j). The circle is relative to the avoided crossing at the SCF level.

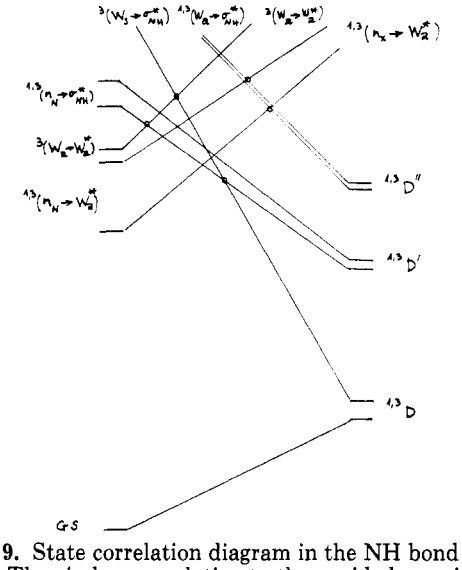

Figure 19. State correlation diagram in the NH bond rupture (path j). The circles are relative to the avoided crossings.

crossing intervenes which assures that no low-lying state of the intermediate II directly correlates with a low-lying state of the fragments.

Since no symmetry elements are preserved along the reaction path, all the resulting crossings will be avoided, yielding maximums along the corresponding PECs.

The calculated curves of Figure 10 describe the whole process of fragmentation in two steps. The barrier which intervenes along the first triplet PEC of the second step (1.2 eV) can be easily overcome if one considers that, at the end of the first step, the system possesses an important internal energy. Its maximal value has been previously estimated at 3 eV.

If the excited singlet valence state is experimentally accessible, the system evolves easily toward fragmentation, the second-step barrier being less than 0.2 eV.

NH Bond Rupture: Path j

During the NH cleavage, the bisecting plane of the CC bond is preserved as a symmetry plane. The natural MO correlation diagram of Figure 18 shows that no HOMO–LUMO crossing occurs. The quasi-degenerate position of the $(n_z + \sigma_H)$ and $(n_z - \sigma_H)$ orbitals is characteristic of a homosymmetric diradical.[21] The lowest states of the fragments are thus the diradical $^{1,3}D$ states. They lie 4.0 eV above the aziridine GS.[29] The $^{1,3}D'$ states which correspond to an excitation from n_x to $(n_z - \sigma_H)$ and the $^{1,3}D''$ states which correspond to an excitation from W_A to $(n_z - \sigma_H)$ come next. The first lies 4.0 eV above the $^{1,3}D$ states and the second 2.0 eV higher.

The state correlation diagram follows (Figure 19). The aziridine GS correlates with ^1D, while S_1, T_1, and T_2 correlate with high excited states $(n_x \rightarrow W_A^*)$ and $(W_A \rightarrow W_A^*)$, respectively. Reciprocally, the ^3D state correlates with a high excited state of aziridine, $^3(\sigma_{NH} \rightarrow \sigma_{NH}^*)$. Avoided crossing results, for the triplet correlation lines.

The calculated curves are represented in Figure 20. They reveal three likely photochemical channels. The first one involves the T_2 triplet state. It requires the overcoming of a weak barrier (0.1 eV) and leads directly to the ^3D state. The second concerns the first singlet S_1 and involves an intersystem crossing at point K. The barrier height (0.25 eV) to reach this point is compatible with the estimated lifetime of such a state. The third concerns the T_1 triplet state. The energy necessary to reach the internal conversion point L is such (0.7 eV) that it is unlikely that the

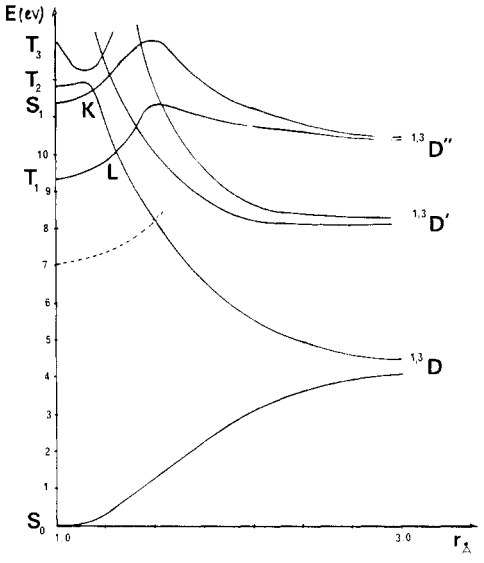

Figure 20. Calculated potential energy curves in the NH bond rupture. The dashed lines are relative to the estimated behavior of the Rydberg state potential energy curves.

system can gain it during its lifetime.

The estimated profile of the Rydberg states' PECs (dashed lines) crosses the dissociative valence PEC at point M. Its position is so high (1.5 eV) that one can estimate the reactivity of the Rydberg states as being very low in the NH bond rupture.

These results lead one to think that the NH bond rupture is not unimolecular in the gas phase but is induced by a radical chain mechanism.

Conclusions

In summary of the detailed study of each potentially reactive reaction path depicted in Figure 1, let us try to present a complete pattern of the photochemical reactivity of the aziridine molecule.

Let us first analyze the gas-phase reactivity. Several hypothesis can be considered. The first one assumes that the valence excited states can be experimentally populated in spite of their very high position. From the S_1 singlet state, the easiest channel is the CN bond rupture ring opening which leads directly to the formation of the intermediate II in its S_1 state (Figure 10). This intermediate may evolve either by fragmentation and formation of

nitrene and ethylene (Figure 10) or by hydrogen migration and formation of methylmethylenimine. This step has not been simulated, but by analogy with cyclopropane,[30] one can consider that it is likely to occur through comparable conditions. It leads to a molecule with a large internal energy, which is likely to dissociate and to yield a methyl radical. This sequence of elementary reactions may constitute the first steps in the formation of the saturated hydrocarbons experimentally obtained.

Other channels from the aziridine S_1 state are the formation of carbene (path e) or nitrene (path h) by simultaneous two-bond scission. The first one involves a decay from the S_1 to the S_0 surface under favorable conditions (Figure 13). The second leads directly to the formation of the fragments, following a PEC which has an inflexion point but is continuously decreasing.

From the T_1 triplet state, every reaction path is likely to occur, and no selectivity is predictable.

The second hypothesis assumes that aziridine is liable to react only from its Rydberg states, experimentally more easily accessible. In this case, only the CN bond rupture appears likely to occur. It leads to the formation of the intermediate II which can evolve as previously described.

In the condensed protic phase, the CC bond reactivity is modified. The disrotatory mode involves an intersystem crossing after overcoming a 0.3-eV barrier (point D, Figure 8). The conrotatory mode leads directly to the intermediate I in its Z_1 state after overcoming a 0.8 eV barrier through a transition state which is near the products. It appears that experimentally the first situation is more favorable than the second. Let us note that intermediate I representes a stable species in its first singlet state, contrary to the corresponding trimethylene in the opening of the cyclopropane.[31] This difference may explain why the diradical can be trapped by cycloaddition in the case of aziridine while it cannot in the case of cyclopropane.

In condensed protic media, the CC bond rupture ring opening can thus compete with the CN bond rupture ring opening, alone likely to occur in gas phase. Let us note that the quantum yield of the former reaction can be strongly reduced since the reverse cyclization reaction is spontaneous, i.e., no barrier prevents it, contrary to the CC bond rupture ring opening.

Registry No. Aziridine, 151-56-4.

(30) J. A. Berson, L. D. Pedersen, and B. K. Carpenter, *J. Am. Chem. Soc.*, **98**, 122 (1976), and references therein.

(31) J. A. Horsley, Y. Jean, C. Moser, L. Salem, R. M. Stevens, and J. S. Wright, *J. Am. Chem. Soc.*, **94**, 279 (1972).

(32) It is clear that our model overemphasizes the influence of hydrogen bonding in protic solvent. Indeed, in the water molecule, the local charge on the hydrogen atom is only +0.3 eV [see, for example, M. S. Gorden et al., *J. Am. Chem. Soc.*, **97**, 1326 (1975)] while we have taken a +1.0 eV value. This crude model has been retained because a more complicated one (several water molecules) should require calculations beyond the scope of this paper in order to eliminate an arbitrary error worse than the lack of precision of the present model.

Substituent Effect Treatment of Interactions between Contiguous Functionalities G–X. 1. Remote Response to Polar and Inductive Influence of X on G = C(sp^3) and –N<

Silvia Bradamante and Giorgio A. Pagani*

Centro CNR and Istituto di Chimica Industriale dell'Universita', 20133 Milano, Italy

Received August 3, 1979

^{1}H and ^{13}C NMR shifts in Me_2SO for molecules of type PhGX and ^{19}F NMR shifts for molecules of type *p*-FPhGX have been evaluated for measuring the direct effect of the substituent X on the contiguous group G (G = CH_2, CH(Ph), NH, O). The sensitivity of the substituent chemical shift (SCS) of the para monitor ^{13}C in α-substituted benzhydryl derivatives Ph_2CHX (**2**) is 0.9 times that of α-substituted benzyl derivatives $PhCH_2X$ (**1**), indicating a negligible partitioning of the substituent effect between the two rings. Para monitor (^{13}C and ^{19}F) substituent chemical shifts in PhNHX, where the X's are substituents capable of only polar-inductive (nondelocalizative) interactions with the NH group, are linearly related with those of **1**, but their sensitivities are more than 2 times greater, indicating that the π-inductive effect plays an important role, together with a mesomeric component effect inductively controlled by the substituent X. SCS's in α-substituted benzyl derivatives **1** are linearly related to the acidities of α-substituted *p*-toluic acids and to ^{19}F SCS's in meta-substituted fluorobenzenes (**6**). SCS's of several substituents in substrates **1–3** are fitted by the reported σ_I values: there are, however, notable exceptions (e.g., the CN substituent) which remain unaccounted for by the DSP (dual substituent parameter) treatment. A basis set of reported σ_I values which originate an excellent correlation for $PhCH_2X$ is defined: hitherto unreported σ_I values are then extrapolated together with new, adjusted σ_I constants for those substituents whose previously reported values were unsatisfactory. The expanded, partially modified σ_{IB} scale gives excellent results with benzhydryl derivatives **2** and with meta-substituted fluorobenzenes (**6**). Reasons for the deviance of the cyano group and for the electron-withdrawing effect of the methyl group are proposed and discussed.

Molecules can be submitted to substituent-effect treatment whenever they present a variable substituent X, an involved (reacting) group G, and a monitor MON as discernible entities.[1] Effects exerted on the group G by a set of substituents X are evaluated by variations of a detector, either a thermodynamic function connected to or a physical property of the monitor. In the thermodynamic approach the detector for substituent effects is represented by the ease (ΔG) or the barrier (ΔG^*) of the bond breaking or bond forming of the bond between the involved (reacting) group G and the monitor, while in the extrathermodynamic approach the detector is a property (e.g., NMR chemical shift) of the same monitor eventually bonded to the group G. Taft and co-workers presented overwhelming experimental evidence for the usefulness of σ constants derived from ^{19}F NMR measures in predicting

(1) (a) L. P. Hammett, "Physical Organic Chemistry", 2nd ed., McGraw-Hill, New York, 1970, Chapter 11; (b) R. W. Taft, *J. Phys. Chem.*, **64**, 1805 (1960).

0022-3263/80/1945-0105$01.00/0